CERN/DRDC/90-50
DRDC/P 11
October 5, 1990

WARM LIQUID CALORIMETRY FOR LHC

E. Geulig, T. Lehmann, W. Wallraff
I. Physikalisches Institut der RWTH Aachen, Germany

A. Bezaguet, F. Cavanna, P. Cennini, S. Cittolin, P. Dreesen, M. Demoulin, L. Dumps, A. Fucci, G. Gallay, A. Givernaud, A. Gonidec, W. Jank, G. Maurin*, A. Placci, J.P. Porte, E. Radermacher, D. Samyn, D. Schinzel, W.F. Schmidt**, B.G. Taylor
CERN, Geneva, Switzerland

E. Pietarinen
Departement of HEP, University of Helsinki, Finland

P. Casoli, S. Centro, F. Dal Corso
Dipartimento di Fisica dell'Università e Sezione INFN di Padova, Italy

P. Carlson, W. Klamra, Th. Lindblad, B. Lund-Jensen,
Manne Siegbahn Institute of Physics, Stockholm, Sweden

* *Contact person*
** *Hahn-Meitner Institut, Berlin*

Abstract

Recent results from the beam tests of the U/TMP "**warm liquid**" calorimeter, constructed by the UA1 Collaboration, show that such a technique is very promising for LHC. Our aim is to extend this programme and design a calorimeter that can satisfy the requirements of high rates, high radiation levels, compensation, uniformity and granularity, as well as fully contain hadronic showers.

We propose to construct liquid ionization chambers operated at very high fields capable to collect the total charge produced by the passage of ionizing particles within times comparable to the bunch crossing time of the future Collider. For this reason we plan to extend the current programme on tetramethylpentane (TMP) to tetramethylsilane (TMSi). Our programme includes irradiation tests of both room temperature liquids to investigate their behaviour as far as pressure increase, electron mobility and electron lifetime is concerned.

As a first step an electromagnetic calorimeter consisting of very high field ionization chambers filled with TMSi as sensitive medium with Uranium and/or other high density material as absorber will be built, on which newly designed fast amplifiers and read out electronics will be tested. In a second step a full scale calorimeter module will be constructed.

In addition, as already agreed for the completion of the UA1 U/TMP activity, a fully assembled supergondola will be installed in ECA 5 in order to test noise and cross-talk in real environment. Cosmic ray runs will allow to control calibration and stability under several conditions over a long period of time.

1. INTRODUCTION

This proposal is directed towards the development of a calorimeter for the future Large Hadron Collider LHC. The main features of the calorimeter are the use of layers of high density material (Uranium or similar) interleaved by ionization chambers, including tracking detectors, filled with room temperature liquid. There are several reasons for which calorimeters based on a liquid detecting medium with high mobility are of considerable interest for a LHC detector, namely the direct relation between charge and energy deposition, the ease of accurate calibration and the possibility of fine transverse and longitudinal segmentation.We have opted for a room temperature liquid as sensitive medium to obtain maximum hermeticity and e/π compensation. In addition, with the exception of Methane, TMSi has by far the highest electron drift velocity at high fields.

In the past several liquids have been studied [1] and the relevant properties are given in table 1. The important parameters are the drift time t_d (fig.1) and the ion pair yield $G_{fi}(E)$ (fig. 2), which we have calculated using Onsager's theory [2]. Neopentane has been included, calculated with the same programme and compared with experimental values [3] in order to check the calculation. As can be seen from fig. 2, at infinite field $G_{fi}(\infty) \approx 4$ which agrees with the gas phase W-value ($W \approx 25$ eV).

Apart from TMP, all the liquids listed in table 1 have nearly the same drift velocity, while the ion pair yield does not vary much. As candidate liquids, tetramethylpentane (TMP) and tetramethylsilane (TMSi) will be considered. These liquids have been investigated intensively in the development of the UA1 calorimeter project [4, 5]. Especially, the production of large volumes of ultrapure liquids giving electron life times of the order of several hundred microseconds (fig. 3) is now well established, as well as the cleanliness of containers and ionization chambers [6, 7]. We exclude tetramethylgermane (TMGe) and tetramethyltin (TMSn) because of their price and toxicity.

1.1. The performance of the UA1 Uranium / TMP calorimeter modules

Several large U/TMP calorimeter modules have been constructed and intensively tested in a beam [7]. The modules are subdivided in six samplings in depth. The first four samplings form the electromagnetic section and consist of 2 mm thick Uranium plates sandwiching TMP filled ionization chambers of 3.3 mm

thickness with a double gap of 1.25 mm liquid. The last two sections consist of 5 mm thick Uranium plates sandwiching the ionization chambers. They are operated at electric fields between 8 and 15 kV/cm and perform well as a combined electromagnetic and hadronic calorimeter. The energy resolutions for electrons and pions were measured and are found to be in agreement with expectation from Monte Carlo studies. The resolution for electrons (fig. 4) is given by :

$$(\sigma(E) / E)^2 = (0.12 / \sqrt{E})^2 + (0.009)^2$$

and for pions (fig. 5) we obtain without correction for lateral shower escape, but unfolding the noise distribution:

$$(\sigma(E) / E)^2 = (0.581 / \sqrt{E})^2 + (0.068)^2$$

This resolution is for one U/TMP module ($\lambda = 2.3$) operated at an electric field of 8 kV/cm combined with the UA1 Iron/scintillator calorimeter ("C" module, $\lambda = 4.5$).

Three U/TMP modules mounted on top of each other to avoid lateral shower escape were measured in the same configuration as described above. The result obtained for the hadronic resolution (fig. 5) is:

$$(\sigma(E) / E)^2 = (0.47 / \sqrt{E})^2 + (0.078)^2$$

The improvement in resolution is due to the higher electric field (12 kV/cm) as well as to the lateral containment of the shower.

The energy resolution given above can also be written in linear form to allow more easily direct comparison with quoted results of other calorimeters:

$$\sigma(E) / E = 0.36 / \sqrt{E} + 0.055$$

Due to this calorimeter configuration, namely the combination of the two types of calorimeters, a sizable constant term is present in the pion energy resolution. The hadron resolution improves significantly with increasing electric field whereas the electron energy resolution varies only slightly. The impact point of the electrons is measured in a position detector [8] located at a depth of 3.4 radiation

lengths. The spatial resolution in the position detector for single electromagnetic showers approaches 1.0 mm for energies greater than 30 GeV.

The electron/pion ratio of the U/TMP module followed by the "C" module is found to be close to 1 (fig. 6). This implies that compensation is observed in a non-uniform sampling calorimeter without sacrificing linearity and electron resolution.

The signal to noise ratio averaged over the six samplings of the UA1 modules is 4.4 using 70 GeV muons. The tower to tower uniformity is better than 1%.

Using the matrix method of Engelman et al [9] we find for energies greater than 50 GeV an e/π rejection ratio of 10^{-4} for an electron identification efficiency of 90% [7]. The position detector used on its own provides a pion rejection factor ≈ 20 for pion energies greater than 10 GeV and with the same electron identification efficiency.

The long term stability of hermetically sealed room temperature liquid calorimeters has been established by monitoring the electron lifetime of the prototype electromagnetic calorimeter over the past four years. Fig. 7 shows the measured lifetimes as a function of elapsed time since filling.

1.2. The parameters for room temperature liquid calorimetry at LHC

From the results mentioned above it is evident that this type of calorimeter is also adequate at LHC energies. However, for the application of this technology to the environment of the Large Hadron Collider, the following factors become important:

- ***Fast response of the ionization chambers***

Due to the high luminosity and the repetition rate of 15 nsec of the LHC, it is desirable to collect the full charge in about the same time. By increasing the voltage and decreasing the gap, a drift time comparable to the bunch crossing time can be achieved. TMSi is therefore a more suitable choice than TMP since its drift time is roughly three times shorter (fig. 1). In such a way the overlap of events due to pile-up will be considerably reduced. Nonetheless the problem of positive ion accumulation remains to be studied at high luminosities.

- *Material of the ionization chambers*

At present, the UA1 calorimeter ionization chambers use only stainless steel and ceramics. Future designs may require the use of other metals and insulating materials. Studies of radiation effects on suitable materials and their interaction with the calorimeter liquid are necessary.

- *Granularity and segmentation*

A compromise has to be found between the size of the cells and their number. In order to keep the pile-up small the cell size in the electromagnetic part should be chosen in first approximation between 3 and 5 Molière radii which in the case of an Uranium calorimeter is approximately 5 cm. This reduces the capacitance of the electrodes by a factor of 4 compared to the ones of the present UA1 calorimeter. The size of the electrodes for the hadronic calorimeter can be made larger.

- *Depth*

In order to fully contain electromagnetic showers the length of the first part of the calorimeter has to be 30 X_0. For the same reason the depth of the hadronic section should be at least 7 interaction lengths [10] (fig. 8).

- *Radiation hardness of the liquid*

The radiation doses at LHC will be several orders of magnitude higher than those at the $p\bar{p}$ collider. Over a period of several years the total accumulated dose received by the chambers is expected to reach 10 Mrad (100 kGy) [11]. Radiolytic decomposition of the liquid is expected and the interaction of these radiolytic products with molecules adsorbed on the electrodes and walls may have an influence on the electron lifetime and ion pair yield. In addition these products may lead to undesirable changes of the dielectric properties of the liquid in the ionization chamber. The electron mobility may be affected as well. The influence of the radiolytic products on the performance of the ionization chamber is not known and has to be studied in detail. It may limit the rapidity interval in which a room temperature liquid calorimeter can be operated at the LHC without in situ refilling facilities.

In order to study these problems and to gain the information necessary for the construction of a warm liquid calorimeter for the LHC we submit the present proposal.

2. DESIGN OF TEST CHAMBERS

A small gap chamber is mandatory to keep the operating voltage below 10 kV and to collect the charge within 15 nsec, especially if one wants to install local intelligence for triggering purposes on each tower. In fig. 1, the relation between electric field and charge collection time is plotted. Fig. 2 shows the number of ion pairs produced as a function of the electric field. High electric fields ensure high electron yields since the recombination is reduced. Positive ion effects are reduced as well since the ion drift velocity is higher. The properties of liquids at very high fields have been studied in TMP up to values of 100 kV/cm with currents less than 1 nA (fig. 9). Given the lack of sensitivity of our instrument, the slope due to the self conductivity of TMP is not observed.

We intend to build test chambers with a multigap structure made of successive metallic grids in one liquid volume. The absorber will be outside the liquid containing chambers as is the case in the UA1 calorimeter. The use of metallic grids leads to reduced surface of the electrodes and will allow - beside other effects which we mention later - easy pumping during bake out. In addition the capacitance of the cells will also be some 15 to 20% smaller than for cells with sheet electrodes.

2.1. The test chambers

In the final design of a calorimeter the liquid is contained in rigid boxes in order to avoid microphonic effects. Initially we plan to build small boxes to study the high field behaviour of the liquid in the desired configuration. Each of these test boxes (fig. 10) is made of a stainless steel picture frame unit of 3 x 6 mm^2 profile. The two covers of 0.5 mm stainless steel are laser-welded on the frame. Inside the box are four multigap structures of 5 grids each. These grids are separated by 1 mm, are 5 x 5 cm^2 in size and 0.1 mm thick (fig. 11). They be either stainless steel or Copper-Beryllium produced by photoetching or even metallized ceramic plates. Their flatness guarantees a constant gap width over the whole surface. The grids are held by insulating spacers which can be made out of ceramics, as a first step. Once the boxes are closed they will undergo for cleanliness purposes the same procedure as the boxes of the UA1 calorimeter modules [12], namely washing with ultra pure water, drying with pure Argon, baking out at 250 °C and then filling with TMP or TMSi. With these first boxes all relevant parameters will be studied.

It is our intention to try other insulating materials which can stand the bake out temperature of 250 °C and are radiation resistant to avoid pollution of the liquid.

Therefore, as a part of the R&D programme, we wish to study together with industry how to mould insulated spacers around the grid to form solid blocks to be mounted inside the boxes described above. All connections will be incorporated in the mould such that the connections to the outside is made by one or two feedthroughs only.

The next step in the programme is the construction of a small calorimeter by assembling 45 boxes with existing 2 mm Uranium plates, equivalent to 30 radiation lengths, for beam tests. The number of free electrons expected from minimum ionizing particles in one of the 4 mm multigap chambers is given by :

$$N_e = 1/2 \times 10^{-2} \times d \times G_{fi}(E) \times dE/dx \qquad \text{[electrons]}$$

where d is the gap and $G_{fi}(E)$ is the free ion pair yield as measured [3] and calculated according to the Onsager theory [2]. We use the approximation by Mozumder [13, 14] in order to calculate the number of free electrons.

Fig. 12 shows the number of electrons N_e as function of the electric field for a gap of 4 mm for the liquids of table 1.

2.2. The calorimeter module

As part of the programme we want to study a full scale U/TMSi calorimeter. In the following we describe the choice of parameters which will determine the layout of the calorimeter module to be constructed.

We consider an electromagnetic section of about 30 radiation lengths and a hadronic one of approximately 7 interaction lengths. This depth ensures that more than 95% of the energy of a 150 GeV shower is absorbed [10] (fig. 8).

In the original UA1 design, one of the reasons to choose Uranium as absorber was its compactness. The test beam results [7] show that Uranium in association with TMP gives an e/π ratio close to unity as well as a good hadronic energy resolution without affecting the electron energy resolution. Furthermore the

lateral dimensions of the shower are a factor two smaller with respect to Lead. Extrapolating from these results we expect for 1 mm thick Uranium plates as absorber an electromagnetic resolution of

$$\sigma(E) / E = 0.09 / \sqrt{E}.$$

In order to minimize the constant term in the hadronic resolution an absolutely uniform hadronic calorimeter has to be built. Presently we plan to use the existing 5 mm Uranium plates. In order to avoid overcompensation the number of Uranium plates has to be determined. With the proposed multigap ionization chambers we aim to reach a hadronic resolution comparable to the one from the UA1 calorimeter modules, namely

$$\sigma(E) / E \approx 0.3 / \sqrt{E}.$$

A small constant term due to the stepping from 1 to 5 mm between the electromagnetic and hadronic sections may remain. We point out that other materials like Copper-Tungsten composites or Molybdenum could be included in the research programme.

An additional feature of the calorimeter will be the built-in tracking detector. In contrast to the UA1 calorimeter which has only one position detector we plan to insert several position sensitive detectors, similar in construction to the one used in the UA1 calorimeter, to measure the shower direction.

It is the aim of this proposal to study by simulation the interplay of these parameters in order to reach the best possible configuration. Presently, the UA1 U/TMP calorimeter has been simulated in detail using the Monte Carlo programme GEANT 3.14. We have used the columnar recombination theory of Kramers [15] to obtain the collected charge from the energy deposited in TMP. A good agreement with the experimental data has been observed, especially on the variation of the e/π ratio with the electric field [16]. We plan to use the same Monte Carlo programme to simulate the behaviour of the proposed calorimeter. To achieve the best possible resolution and compensation, the simulation studies must also optimize the choice of the absorber material, its thickness, the cell size of the ionization boxes and the sampling fraction.

Once the parameters are chosen a full scale module will be built and tested. We expect that the test calorimeter will have a 0.5 x 0.5 m^2 cross section. With the experience gained from the 45 box prototype we envisage a similar construction and try to resort to existing material. This test calorimeter will have few hundred detector planes. For practical reasons it will be divided into several segments.

3. ELECTRONICS FOR A WARM LIQUID CALORIMETER

Front-end amplifiers suitable for LHC calorimeters, based on ionization chambers, must satisfy at the same time many demanding requirements. At TeV energies and high luminosities the amplifiers must withstand very high counting rates maintaining simultaneously excellent stability and very large dynamic range. A relevant paper [17] has discussed the " *limit to the counting rate posed by the time required to transfer the charge from the electrodes into the amplifier* ". This time is essentially a function of the length of the connection between the electrode and the amplifier. We propose to study front-end amplifiers which can be mounted very close to the electrode.

3.1. Current integrator

A hybrid current integrator has been designed for the U/TMP calorimeter [5]. The basic characteristics of this component are high transconductance (160 mS), linearity better than 1 ‰ and dynamic range in excess of 5000.

The amplifier was designed for a charge collection time of ≈ 400 ns and a detector capacitance of 1 nF to 8 nF. The high transconductance of the chosen j-FET of the amplifier gives a measured noise slope of 1.2 e/pF.

We are aware that the requirements for this project exceed by far the parameters described above, nevertheless we believe that a suitable charge integrator can be made taking advantage of the new components coming from the growing market of consumer electronics (HDTV). In order to maintain a reasonable signal to noise ratio and to take full advantage of the short charge collection time we have to increase considerably the transconductance/bandwidth ($f_t = k \times g_m/C_{in}$). Moreover, the mechanical structure of the proposed detector will allow the mounting of the amplifiers close to the feedthroughs in order to minimize transit time effects.

3.2. Voltage amplifiers

In contrast to the present U/TMP calorimeter the proposed detector gives access to both, anode and cathode, which will allow the reading of the ionization current as well as its image.

In this new scenario we plan to develop wide-band voltage amplifiers which elaborate the signal obtained by the current integrated on the anode of the detector itself, hence producing an output signal of similar shape as the current pulse in the chamber. Simulation of this type of amplifiers has already been done. The results are promising and we believe that amplifiers with gain-bandwidth product of the order to 10^9 can be obtained. In fig. 13a the SPICE simulated response is given for such an amplifier. It shows a gain of 32 dB with a frequency cut at 580 Mhz. In fig. 13b the response with feedback shaping is given. It shows a comparable gain at 30 Mhz and a cut at 250 Mhz. All simulations assume an input detector capacitance of 400 pF. In fig. 14 the shaped output signal for a triangular input current, 15 ns long equivalent to 1.5 pC is given. The peak appears at 13 ns, the input equivalent noise charge is 5.5 fC.

With such a level of noise the muon calibration of the calorimeter will be difficult to perform. We are presently investigating the possibility of using the integrated cathode current for this purpose. The amplifiers of the U/TMP calorimeter seem adequate for this approach.

3.3. Digital electronics

In parallel with complementary R&D activities on calorimetry for LHC, we propose the implementation of digital front-end electronics comprising high-speed analogue-to-digital converters as well as pipelined digital signal processors for the first and second level trigger systems.

In order to identify possible problem areas and gain experience with the basic elements of a digital front-end readout we propose to develop and use personal computer-based "test benches". These "test benches" will exploit the prototype VLSI systolic array and data-flow processors currently developed in national research laboratories and by the emerging European HDTV industry. These efforts would also lay the foundations for projects involving development of custom designed VLSI circuits.

4. RADIATION HARDNESS OF THE LIQUIDS

4.1. Radiolysis and its influence on electron life time

Radiation energy absorbed by the liquid is converted into ionization and excitation. The energy for the formation of one ion pair is approximately 45 eV at 100 kV/cm. Since the ionization potential of the liquids under consideration is approximately 10 eV, the difference will go into excitation. In a liquid most ion pairs are generated in close spatial correlation and they undergo geminate recombination after a very short half life time. The recombination energy is converted into excitation as well, which is responsible for the breakage of chemical bonds.

Radiolysis of liquid hydrocarbons by γ-radiation or fast electrons has been studied extensively [18]. Usually many products are formed and it is only possible to detect the most prominent ones. The main products which interest in the present context are gases like hydrogen and methane, high molecular weight compounds and radicals which are chemically reactive species with a limited life time. The production of hydrogen and methane may lead to an unwanted increase in pressure. In addition they may form OH^- or H_2O with the oxygen layers on the surface of the walls. These, in turn, may react with the hydrocarbon radicals to form electronegative impurities reducing the electron life time, mobility and yield. It is this one of the main reasons to use grids instead of solid metal electrodes, since their surface is increased by a factor 20 compared to grids. Furthermore, the dissolved gases will take part in further radiolysis reactions. It is one of the objectives of the present proposal to study the effect of high doses on the changes in volume and pressure of TMP and TMSi. The design parameters for the future warm liquid calorimeter will be obtained from the results of these studies.

Appendix I describes in more detail the mechanisms of the pertinent radiation chemistry.

4.2. Dielectric properties

The formation of high molecular weight compounds may influence the electric properties of the ionization chamber. Charge transfer from parent positive ions to dimer or polymer ions reduces the overall mobility of the positive species. This effect may be detrimental to the fast clearing of the gap from positive charges. By drift, the polymer ion is transported to the cathode where it is deposited. An

electrically insulating layer is the result. Such effects have been observed in n-hexane, where the chemical bonds were broken by induced partial discharges [19]. Studies of the changes of dielectrical properties due to the high doses shall be investigated as well.

4.3. New construction material

In the development of the UA1 calorimeter the choice of materials was restricted to ceramics as insulating material and stainless steel for the electrodes and walls. Other requirements for the LHC calorimeter may necessitate the additional use of other materials. The adsorbed molecular layers may differ from on type of metal to another. This will influence the chemistry occuring between radiolysis products and surface. Organic insulating materials are decomposed by radiation and products may be released into the liquid volume. In addition radicals formed in the liquid will react with the insulator surface. It is the aim of this study to identify materials which are suitable for the construction of the ionization chambers of the LHC calorimeter.

4.4. Experimental requirements

During the development of the UA1 calorimeter several ionization chambers were constructed allowing to test various properties of warm liquids, as for instance, electron life time, electron mobility and free electron yield. Long term stability tests have been carried out as well. Two large purification systems have been set up for the UA1 calorimeter project. The principle of purification has been tested successfully on several other liquids like Argon [20] and Xenon yielding lifetimes of 10 msec in Argon and several 100 μsec in Xenon. Adaptation of the present purifier to TMSi does not involve any changes in the system.

In addition, in order to study the influence of high radiation doses on warm liquids we foresee to build special stainless steel containers. In order to avoid pressure increase due to gas pockets, care has to be taken that no gas volume is on top of the liquid, especially close to the valve. The first test consists in measuring a possible pressure increase due to the formation of hydrogen during the irradiation. Next, the irradiated liquid will be transferred into a special counter with double grids where the ionization electrons will be produced with the help of a Laser light irradiating the cathode. The electrons will drift to the anode and the total charge will be measured. Comparing this charge with the one obtained from non irradiated liquid gives directly the decrease in life time due to the radiation.

With Q_0 being the charge produced by photoeffect on the cathode, and Q the charge arriving at the anode we obtain the following relation from where the lifetime τ is calculated:

$$\frac{Q}{Q_0} = e^{-\frac{t_d}{\tau}}$$

Irradiation facilities exist at CERN at the neutrino target and the antiproton target. Use can also be made of the 20 kCi ^{60}Co γ - source at the Hahn-Meitner Institut Berlin. Chemical analysis of radiolysis products is possible by gaschromatography (HMI) or mass spectrometric analysis (CERN).

5. TEST OF A SUPERGONDOLA IN THE UA1 DETECTOR

The construction of 16 modules for one Supergondola, as already agreed for the completion of the UA1 U/TMP calorimeter activity, is well under way. At the present moment 10 modules are filled, of which 3 have been tested intensively at the SPS test beam. In the near future, after the filling of 6 more modules the mounting in the Supergondola structure will start. The assembly including the final cabling and testing will be finished in late autumn. The installation of the completed Supergondola in ECA 5 will follow. All heavy gear for the installation in the magnet is ready and has already been used.

Electronics and read out chain can be checked with test pulses. Noise and cross-talk can be measured and minimized by studying different ground connections. All studies will be performed under different conditions, e. g. with the magnet off, with water cooling on but power off and with the magnet on. An additional parameter which will be varied is the H.V. applied to the ionization chambers. Replacing the old preamplifiers with the new ones having a larger bandwidth a comparative study of noise and cross-talk can be performed.

Stability, linearity and calibration can be intensively studied under the above mentioned conditions over a sufficiently long period of time.

The current UA1 data acquisition must be adapted to meet the requirements for the test of the Supergondola. The readout must be rearranged and upgraded such to allow the test of new front-end implementations. The new

architecture should provide the kernel for future development stations and data acquisition systems.

Depending on the Gondola test results and taking advantage of the existing equipment and material, we do not exclude to forward at a later stage a new proposal to assemble a few Supergondolas based on simple physics motivations.

6. TIME TABLE, RESPONSIBILITIES AND REQUESTS

6.1. Time table

Autumn 1990 :

- Completion of the 16 U/TMP modules, filling and cabling.
- Construction and cabling of one Supergondola.
- Design study of small test chambers and preliminary test of components.
- Specifications for new fast electronics.
- Design and construction of containers for irradiation tests.
- Construction and test of the Laser ionization chamber.
- PS test beam measurements of UA1 U/TMP modules.

Beginning 1991 :

- Installation and test of the Supergondola in the UA1 magnet.
- Construction and test of small chambers.
- Prototypes design and test of new fast electronics.
- Irradiation of TMP, TMSi and new materials with subsequent life time measurements.
- Simulation studies for a full calorimeter unit.

Summer 1991 :

- Continuation of irradiation tests.
- Construction of small calorimeter modules.

1992 :

- Test of small calorimeter modules with new electronics.
- Continuation of irradiation tests if necessary.
- Design and engineering study of a full scale calorimeter module.

6.2. Responsibilities

Aachen : - Participation in the preparation, design and construction of the containers and Laser ionization chamber for the irradiation tests.
- Participation in the irradiation tests and the subsequent analysis.

CERN : - Coordination of the beam test activities.
- Participation in mechanical design studies.
- Construction of small test chambers.
- Construction and test of the Supergondola in ECA5.
- Participation in preparation and irradiation tests.
- Design of the data acquisition system.
- Simulation studies.

Helsinki : - Participation in the data acquisition system.

Padova : - Design and construction of new fast electronics and digital front-end.

Stockholm : - Participation in the purification system.

We are presently discussing with physicists of Imperial College, London, in order to extend the collaboration.

We also envisage a common effort with College de France, Paris, on the basis of their proposal to be submitted to the DRD Committee [23].

6.3. Requests

- Test beam request :

Additional measurements of the UA1 U/TMP modules are necessary starting from spring 1991. As soon as the new small test chambers will be ready a beam test will be performed. We propose to test our modules and prototypes in the X1 beam (West area) where our previous tests were carried out. The equipment used for our 1990 test is still installed and ready to be operated. We request 2 months of test beam per year.

For irradiation tests (AA/LEAR target) we request 2 times 6 months starting in 1990, 1991 and part of 1992.

- Computer time request :

During the year 1990, 16 000 hours (IBM units) on the CRAY computer were allocated to UA1, essentially used for the UA1 upgraded calorimeter studies (simulation and test beam analysis). In order to perform the same type of Monte Carlo simulation we request the same computing time on the Cray for 1991 and 1992.

- Budget request to CERN for years 1991 and 1992 :

• Prototype chambers	100 KSF
- design study	
- prototype construction	
• Small calorimeter module for beam test	250 KSF
- design and construction (45 chambers)	
• Electronics and DAQ	250 KSF
- Front end preamplifiers	
- processing unit prototypes	
- test benches integration	
• Irradiation tests	50 KSF
- design and construction of container	
- laser ionization chamber	
- test setup	
- Laser source (on loan ??)	
• ECA5 Supergondola test	50 KSF
- DAQ	
- installation	
- electronics	

- Test beam equipment 60 KSF
  - electronics pools
  - computers maintenance

- Travel budget, (25 KSF per year, 1991 and 1992) 50 KSF

- Contract labour manpower
  - R&D activities, (80 KSF per year for 2 years) 160 KSF

The total budget request amounts to 970 KSF and is equally shared between 1991 and 1992.

- Manpower status :

When we will reach the study and design phase of a full scale calorimeter unit an adequate technical support, CAD oriented, will be mandatory. An addendum to the present proposal will be forwarded to the relevant Committee.

7. APPENDIX I : Radiation hardness of the liquids

7.1. Radiolysis

Radiation energy absorbed by the liquid is converted into ionization and excitation. The energy for the formation of one electron-positive ion pair is approximately 45 eV at fields of interest. Since the ionization potential is around 10 eV, about 35 eV go into direct excitation. In a liquid most electron/positive ion pairs are generated in close spatial correlation and they undergo geminate recombination after a short half lifetime, which is of the order of several picoseconds. The recombination energy is converted into excitation as well. It is the total excitation energy which leads to the breakage of chemical bonds. In hydrocarbons the following average bond energies are important (Tab. I):

Table I: Average bond energies

Bond	[kcal/mole]	[eV]
C - C	83	3.6
C - H	99	4.3
CH_3 - M	80 - 90	3.5 - 3.9

The main results of bond breakage is the formation of radicals R. Radicals are chemically reactive species with a limited life time. They disappear either by reaction with molecules M of the liquid or by reaction with each other:

$$R + M \xrightarrow[k_s]{} \text{products} \qquad \text{(I)}$$

$$R + R \xrightarrow[k_r]{} R_2 \qquad \text{(II)}$$

The balance of radical production and disappearance can be written as

$$d[R] / dt = k_g \times D_r - k_s \times [R] - k_r \times [R]^2,$$

where the k's are reaction constants and the brackets denote the concentration.

The first term on the right hand side is the generation term. It is proportional to the dose rate D_r. The second term describes reaction (I), a first order reaction while the second term describes reaction (II), a second order reaction. Low dose rates favour first order reactions while high dose rates favour second order reactions. This argument may be even extended to the influence of the linear energy transfer (LET) of the radiation in such a way that the spatial deposition of radicals by low LET radiation is equivalent to a low dose rate while high LET radiation produces locally a high dose rate. The yield of a particular chemical product produced by radiolysis is naturally a function of the total dose absorbed but in addition it is a function of LET and dose rate.

In order to compare different experimental data the product yield is usually given as the G-value which denotes the number of species (radicals, ions, electrons) produced per 100 eV of absorbed energy. This energy is expressed in SI units, namely in Gy = 1 J/kg (Gy = Gray). The radiation absorbed dose is expressed in rad, 100 rad = 1 Gy or in eV/g, 1 rad = 6.24 10^{13} eV/g.

Radiolysis of liquid hydrocarbons by γ-radiation or fast electrons has been studied quite extensively [18]. Usually many products are formed and it is possible only to detect the most prominent ones. Experiments are carried out with the degassed liquid in a sealed ampoule with a vapour space. After a given dose the gas phase is pumped off and the composition is determined by mass spectrometry or gaschromatography. Substances dissolved in the liquid are identified by gaschromatography. Insoluble substances are characterized by analysis of the elements. The G-values derived for the various products are obtained from experiments where the product yield is proportional to the absorbed dose. As the irradiation proceeds the products formed initially enter into the radiolytic reaction and deviations from this proportionality occur.

The main products which are of interest in the present context are the gases hydrogen and methane and high molecular weight compounds. The detailed G-values for a specific liquid and radiation can be found in the literature [18]. Here we will concentrate on discussions which require orders of magnitude only. In the following table II we have compiled the necessary G-values.

Table II: Approximate G-values for hydrocarbons and low LET radiation

Product	G-values [species/100 eV]	
	n-alcane	branched alcane
hydrogen	5	2
methane	0.2	1
unsaturates	0.5	
$\geq C_{2n}$	1-2	
Degradation	10	10

The amount of a particular substance formed in a volume V by the absorption of a given dose D [eV/ l] is calculated as the number of species N_0,

$$N_0 = G \times 10^{-2} \times D \times V$$

Division by the volume and Avogadro's number $N_A = 6 \times 10^{23}$ gives the concentration in moles per liter,

$$[S] = G \times 10^{-2} \times D / N_A$$

As an example we will calculate the concentration of hydrogen formed by an absorbed dose of 10 Mrad = 6.24×10^{20} eV/g. Assuming a liquid density $\rho = 0.7$ g/cm^3, a dose of 4.4 10^{23} eV/l is obtained. For G = 5, $[H_2]$ = 36 millimoles per liter, and for G = 2, $[H_2]$ = 14.7 millimoles per liter is obtained. A total of 72 millimoles of liquid molecules are destroyed per liter. Since there are approximately 7 moles of liquid per liter (M_w = 100), 1% of the liquid molecules has been changed.

7.2. Solubility and pressure

The following considerations are for a model branched hydrocarbon (TMP, TMSi, Neopentane) where hydrogen and methane are the main gaseous products. The solubility of a gas is usually described by Ostwald's solubility coefficient L which is given by the ratio:

L = [gas concentration in the liquid phase] / [gas concentration in the vapour phase].

For small non-polar molecules as H_2 and CH_4, L is smaller than 1. The solubility coefficient for H_2 and CH_4 is assumed to be 0.1 and 0.4 respectively.

In presence of a vapour space a higher concentration of hydrogen will develop in the vapour space leading to an increase in pressure. Assuming $G(H_2) = 2$, 14.7 millimoles per liter are generated for 10^7 rad. The concentration in the vapour phase will increase to 147 millimoles per liter. The pressure built-up depends on the volume of the vapour space. Assuming a volume of 1 % (i.e 10 cm^3) of the liquid volume the amount of hydrogen in the vapour space is 1.47 millimole. Since 1 bar corresponds to 0.446 millimoles, the resulting pressure increase would be 3.3 bar. An additional pressure contribution comes from the methane generated. With $G(CH_4) = 1$, 0.4 bar is obtained. The total pressure would be 3.7 bar. Note that these estimations may be scaled up or down when the correct data for G and L are available.

In absence of a vapour space, the equivalent pressure exerted by the H_2 molecules (assuming G = 2) is p = 330 mbar. The formation of micro bubbles of hydrogen may take place but this process is yet to be established. It is possible that the hydrogen remains dissolved in the liquid without forming a vapour phase. This process will depend on the overall volume change which is due to the disappearance of liquid molecules and the formation of the product molecules. Furthermore, if the liquid contains no vapour space the dissolved gases will take part in the radiolysis reactions.

7.3. Electron life time and mobility

The electron life time is limited by the concentration of electronegative substances present in the liquid. These are compounds containing O, F, Cl, Br, I atoms. Although the liquid will have a very low level of these compounds, radiation chemical effects may transport substances adsorbed at the electrodes and the walls into the liquid. Water and oxygen are certainly adsorbed. Radicals formed by radiation near the walls may react with O_2 or H_2O and potentially harmful compounds are thus transported into the liquid. Removal of these adsorbed layers before final filling seems necessary. Another group of compounds which may influence the electron life time are unsaturated compounds formed during the

radiation. Although very little data exist in the literature, it may be concluded from previous experience that a finite attachment probability exists. With a G-value of 2 we obtain 14.7 mM/l for [C=C]. Since the life time τ is given by

$$\tau = ([S] \times k_S)^{-1},$$

[S] being the scavenger concentration, we obtain for a reaction constant $k_S = 10^6$, $\tau = 68$ μsec and for $k_S = 10^9$, $\tau = 68$ nsec.

The mole fraction of foreign species formed during radiolysis is approximately 0.01. Such a concentration is expected to have a small but non negligible effect on the mobility. In mixtures of liquid methane and ethane [21] it was found that 1 mole percent of ethane reduced the electron mobility in methane by approximately 8 %. A similar effect may be expected for the free ion yield.

7.4. Dielectric properties

The formation of high molecular weight compounds may influence the electric properties of the ionization chamber.

Charge transfer from parent positive ions, M^+ to polymer ions, M_n^+ reduces the overall mobility of the positive species,

$$M^+ + M_n \text{ --------> } M_n^+ + M$$

This effect may be detrimental to the fast clearing of the gap from positive charges. By drift, M_n^+ is transported to the cathode where it is deposited. An electrically blocking layer is the result. Such effects have been observed with partial discharges in n-hexane [19]. Deposition on insulator surfaces may lead to changes in the dielectric strength.

8. REFERENCES

[1] W. F. Schmidt, Can. J. Chem. **55** (1977), 2197.
T. G. Ryan and G. R. Freeman, J. Chem. Phys. **68** (1978), 5144.
H. Jungblut and W. F. Schmidt, Nucl. Instr. and Methods **A241** (1985), 1128
J. Engler, H. Keim and B. Wild, Nucl. Instr. and Methods **A252** (1986), 29.
H. Faidas, L. G. Christophorou, D. L. McCorkle and J. G. Carter, submitted to Nucl. Instr. and Methods.
S. Geer, R. A. Holroyd and F. Ptohos, Nucl. Instr. and Methods **A287** (1990), 447 and BNL 44709, June 1990.
I. Lopes and W. F. Schmidt, Z. Naturforsch. **45a** (1990), 832.

[2] L. Onsager, Phys. Rev. **54** (1938), 554.

[3] W. F. Schmidt, Radiation Research **42 (1970),** 73.

[4] M. G. Albrow et al., Nucl. Instr. and Methods **A265** (1988), 303.

[5] C. Bacci et al., Nucl. Instr. and Methods **A292** (1990),113.

[6] A. Gonidec, C. Rubbia, D. Schinzel and W. F. Schmidt, CERN - EP/88 -36.

[7] R. Apsimon et al., to be published.

[8] K. Ankoviak et al., Nucl. Instr. and Methods **A279** (1989), 83.

[9] R. Engelmann et al., Nucl. Instr. and Methods **216** (1983), 45.

[10] M. Abolins et al., Nucl. Instr. and Methods **A280** (1989), 36.

[11] G. R. Stevenson and H. Schönbacher, CERN 88-02 (1988), 39.

[12] Design report of a U/TMP calorimeter for the UA1 experiment with ACOL, UA1 TN/86-112 (1986).

[13] A. Mozumder, J. Chem. Phys. **60** (1974), 4300.

[14] H. Jungblut, Diplom thesis, Fachberich 20, Freie Universität Berlin (1975).

[15] H. A. Kramers, Physica **18** (1952), 665

[16] A. Givernaud, Proceedings of the ECFA study week on Instrumentation Technology for High-Luminosity Hadron Colliders, Barcelona September 1989, CERN 89-10, Vol. 2, 551

[17] V. Radeka and S. Rescia, Nucl. Instr. and Methods **A265** (1988), 228.

[18] A. J. Swallow, Radiation Chemistry of Organic Compounds, Pergamon Press, Oxford, 1960

[19] J. Fuhr and W. F. Schmidt, IEEE Trans. on Electrical Insulation **EI-23** (1988), 485

[20] E. Buckley et al, Nucl. Instr. and Methods **A275** (1989), 364.

[21] G. Bakale, W. Tauchert and W. F. Schmidt, J. Chem. Phys. **63** (1975), 4470

[22] R. K. Böck, T. Hansl-Kozanecka and T. P. Shah, Nucl. Instr. and Methods **186** (1981), 533.

[23] L. Dobrzynski, D. Kryn, D. Marchand, J.P. Mendiburu, P. Salin, "The Prism Plastic Calorimeter", Proposal to be submitted to the DRD Committee.

Table 1 : CHARACTERISTICS OF WARM LIQUIDS

	TMP	TMSi	TMGe	TMSn
Formula	C_9H_{20}	$C_4H_{12}Si$	$C_4H_{12}Ge$	$C_4H_{12}Sn$
Density [g / cm^3]	0.72	0.645	1.006	1.314
Dielectric constant	1.98	1.92	2.01	2.25
Radiation length [cm]	62.3	52.2	18.2	9.2
dE / dx [MeV / cm]	1.58	1.36	1.78	2.09
Mobility μ_e [cm^2 / V.sec]	30	100	90	70
Drift time t_d [nsec] at 50 kV / cm for 1 mm gap	74	23	23	24
Ion pair yield G_{fi} (0) per 100 eV at zero field	0.75	0.63	0.61	0.63
Flashpoint [°C]	7	-18		
Boiling point [°C]	123	27	43	78
Vapor pressure [Torr] at 20 °C	15	650		

9. FIGURE CAPTIONS

Fig. 1 : Drift time in TMP, TMSi and TMSn as a function of the electric field applied to a 1 mm gap ionization chamber.

Fig. 2 : Ion pair yield per 100 eV in TMP, TMSi, TMPGe, TMSn and Neopentane as a function of the electric field. The dotted points are experimental values taken from reference [3].

Fig. 3 : Typical waveform obtained with cosmic rays. The measured points are well reproduced by the theoretical curve. The upper curve gives the rise time and the lower one the decay time.

Fig. 4 : Electron resolution of the UA1 U/TMP calorimeter modules as a function of the reconstructed beam energy.

Fig. 5 : Hadronic resolution of the UA1 U/TMP calorimeter modules as a function of the reconstructed beam energy for two running conditions.

Fig. 6 : Ratio of the reconstructed electron to pion energies for the UA1 U/TMP calorimeter as a function of the incident particle energy for two running conditions.

Fig. 7 : Measured lifetime in the UA1 TMP prototype calorimeter over a period of 4 years.

Fig. 8 : Longitudinal shower containment as a function of the number of interaction lengths traversed by the shower. The curves are the predictions of the parametrizations of Böck et al. [22]. The data points are from reference [10].

Fig. 9 : Current in TMP versus the electric field.

Fig. 10 : Layout of an ionization chamber.

Fig. 11 : Grid electrodes with insulating spacers.

Fig. 12 : Number of electrons in TMP, TMSi, TMSn and TMGe as a function of the electric field in a 4 mm multigap chamber

Fig. 13a : SPICE simulated response for a wide-band voltage amplifiers.

Fig. 13b : Response of the amplifier with feedback shaping.

Fig. 14 : Shaped output for a triangular input current.

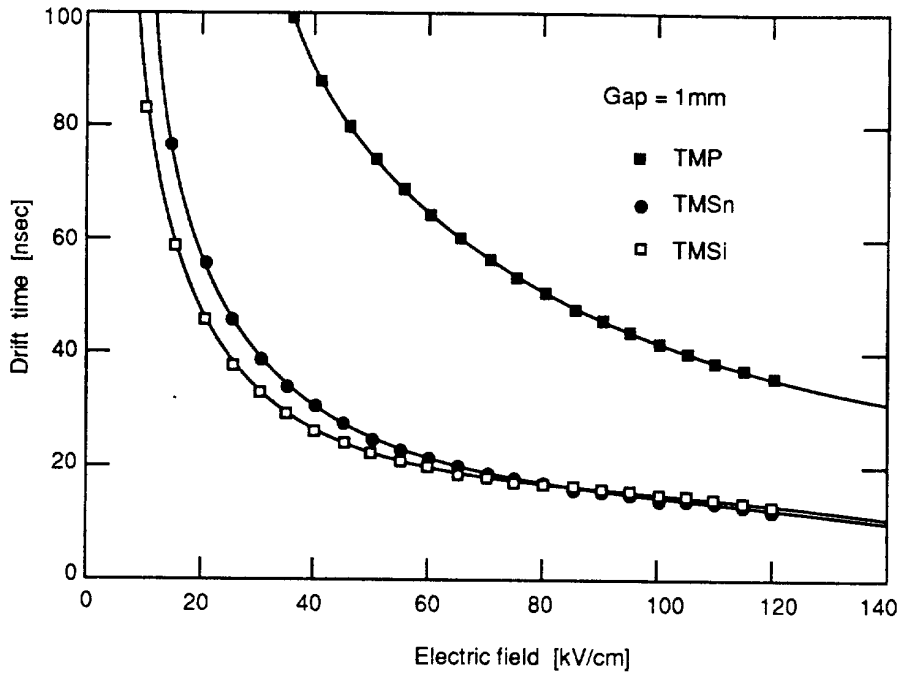
Gap = 1mm
TMP
TMSn
TMSi
Drift time [nsec]
Electric field [kV/cm]
0
20
40
60
80
100
120
140

Fig. 1

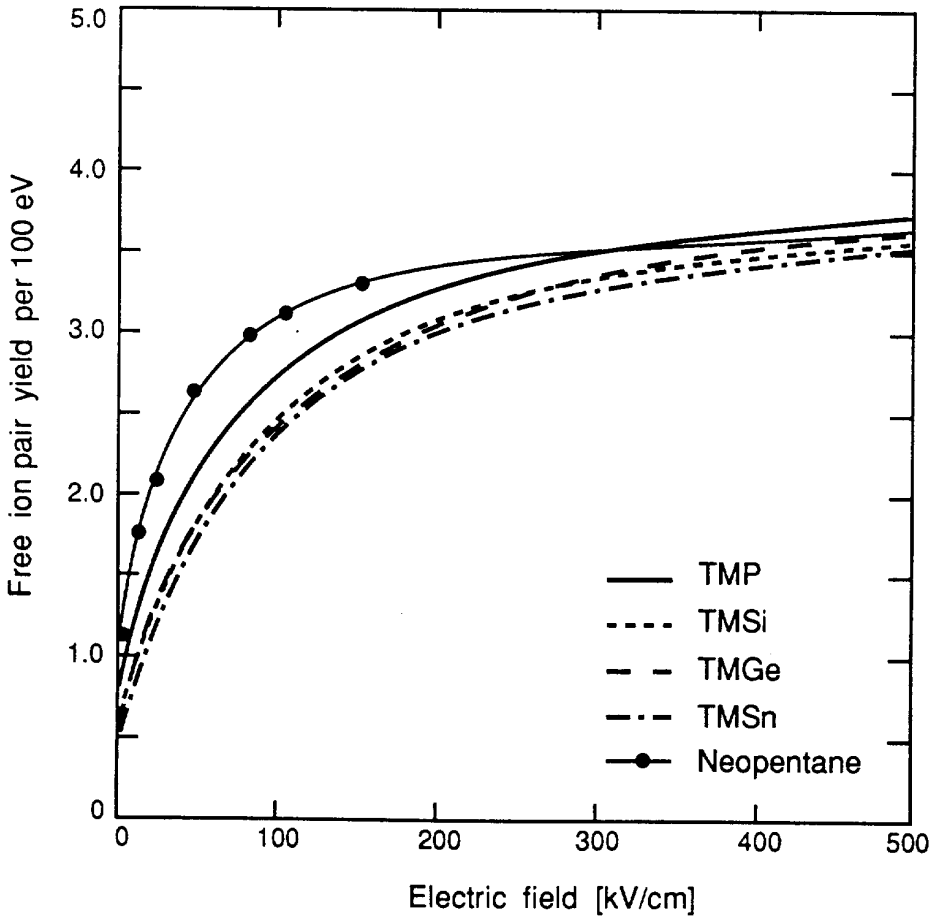
TMP
TMSi
TMGe
TMSn
Neopentane
Free ion pair yield per 100 eV
Electric field [kV/cm]
0
1.0
2.0
3.0
4.0
5.0
100
200
300
400
500

Fig. 2

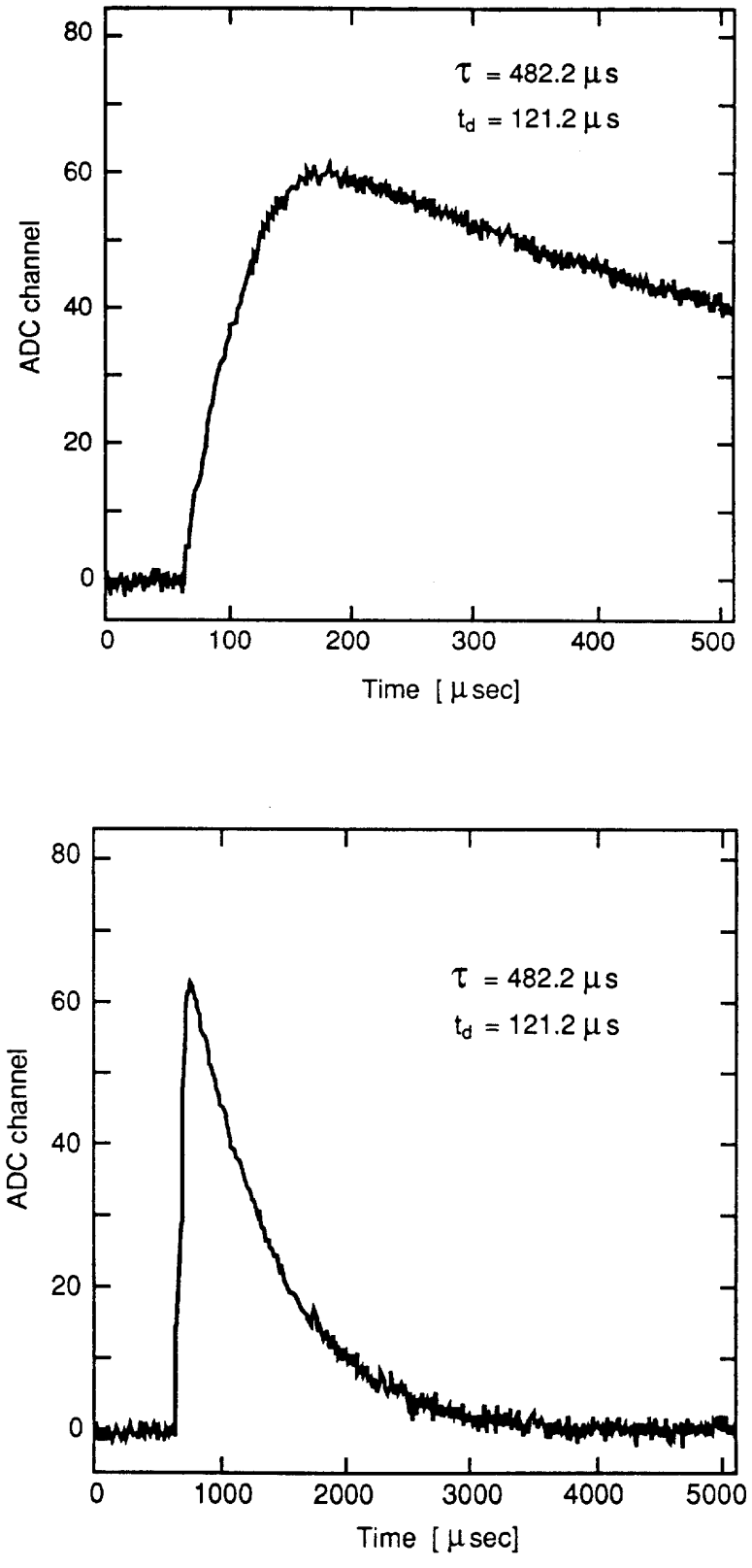
τ = 482.2 μs
t_d = 121.2 μs
ADC channel
Time [μsec]
0
20
40
60
80
0
100
200
300
400
500
τ = 482.2 μs
t_d = 121.2 μs
ADC channel
Time [μsec]
0
20
40
60
80
0
1000
2000
3000
4000
5000

Fig. 3

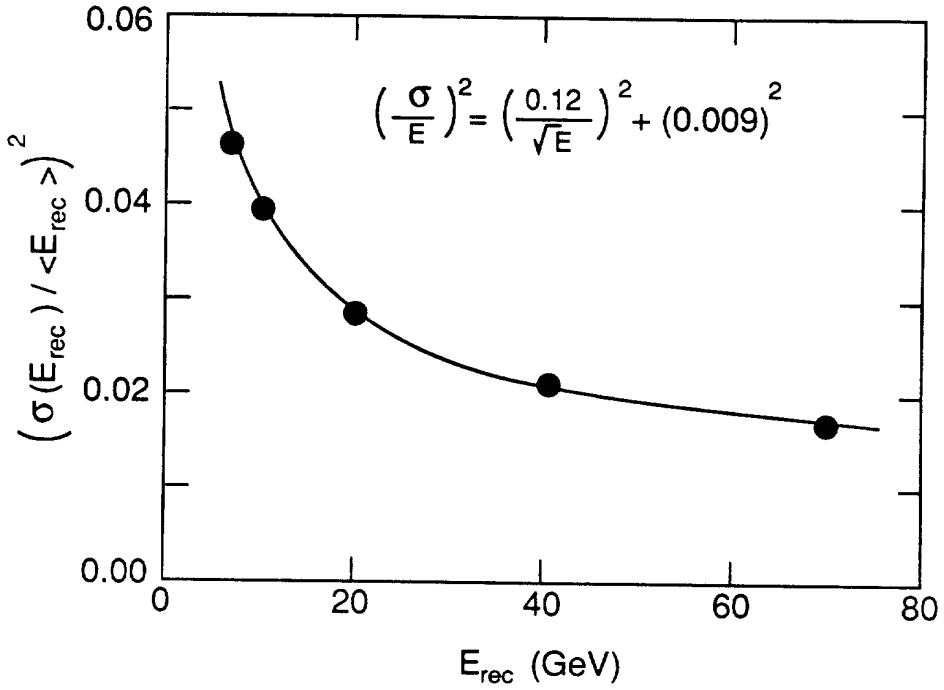
0.06
0.04
0.02
0.00
0
20
40
60
80
$\left(\frac{\sigma}{E}\right)^2 = \left(\frac{0.12}{\sqrt{E}}\right)^2 + (0.009)^2$
$\left(\sigma(E_{rec}) / \langle E_{rec} \rangle\right)^2$
E_{rec} (GeV)

Fig. 4

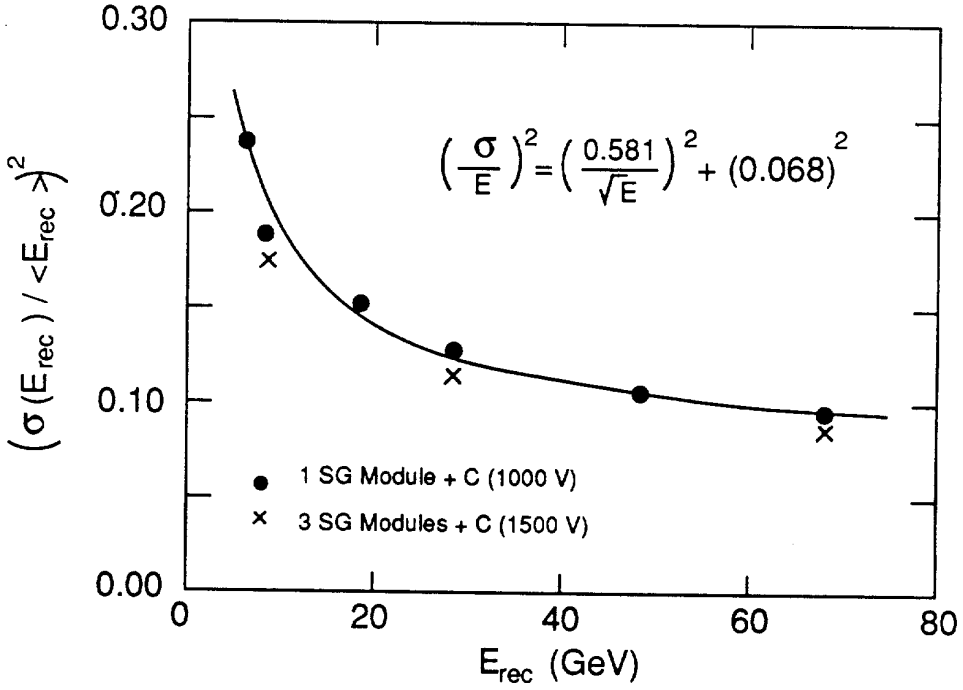
0.30
0.20
0.10
0.00
0
20
40
60
80
$\left(\frac{\sigma}{E}\right)^2 = \left(\frac{0.581}{\sqrt{E}}\right)^2 + (0.068)^2$
1 SG Module + C (1000 V)
3 SG Modules + C (1500 V)
$\left(\sigma(E_{rec}) / \langle E_{rec} \rangle\right)^2$
E_{rec} (GeV)

Fig. 5

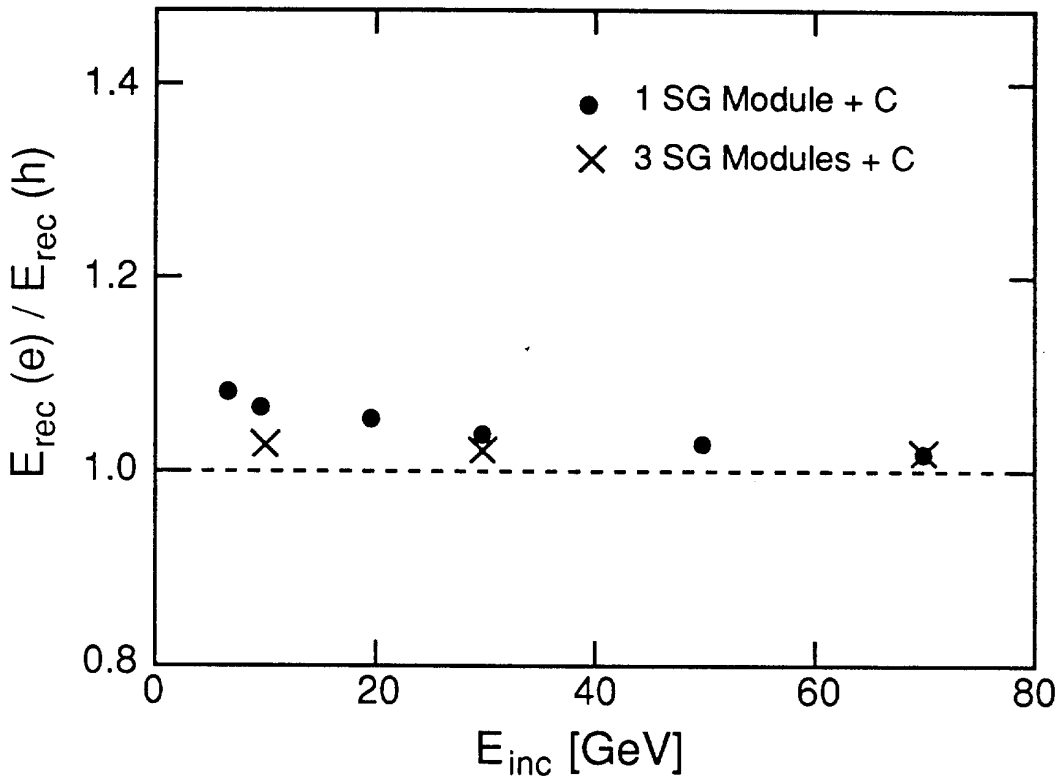
1.4
1.2
1.0
0.8
0
20
40
60
80
E_{rec} (e) / E_{rec} (h)
E_{inc} [GeV]
1 SG Module + C
3 SG Modules + C

Fig. 6

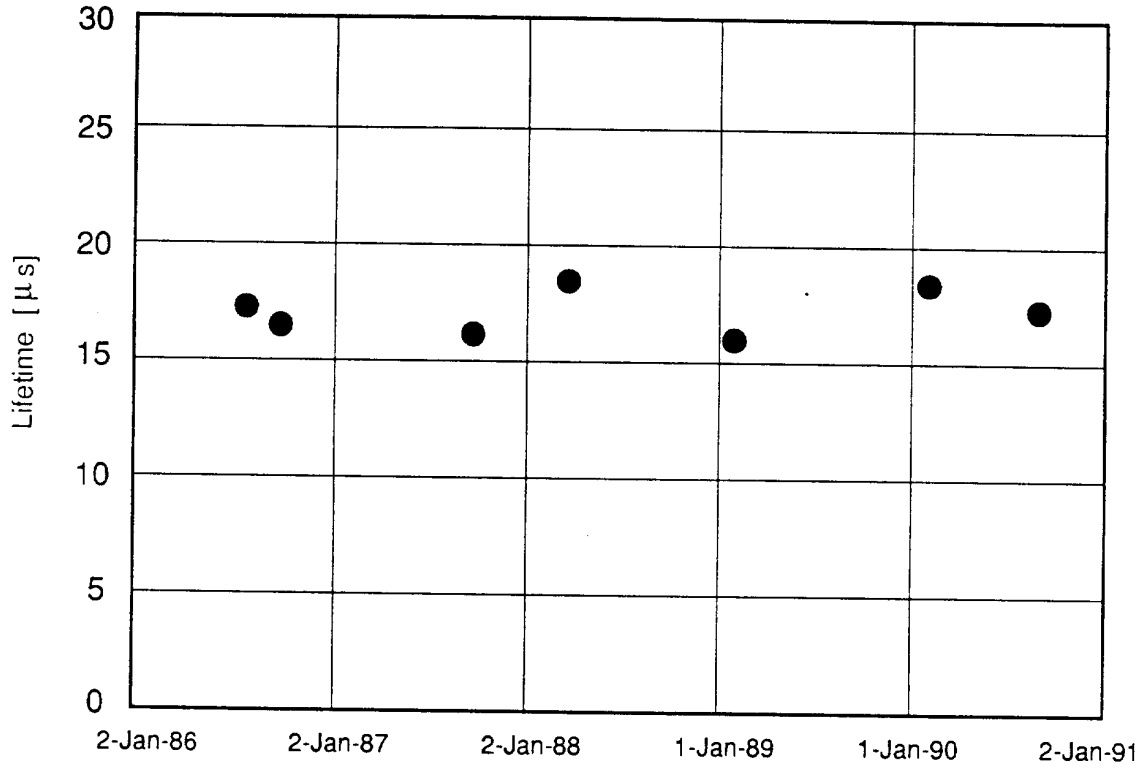
30
25
20
15
10
5
0
Lifetime [μs]
2-Jan-86
2-Jan-87
2-Jan-88
1-Jan-89
1-Jan-90
2-Jan-91
Date

Fig. 7

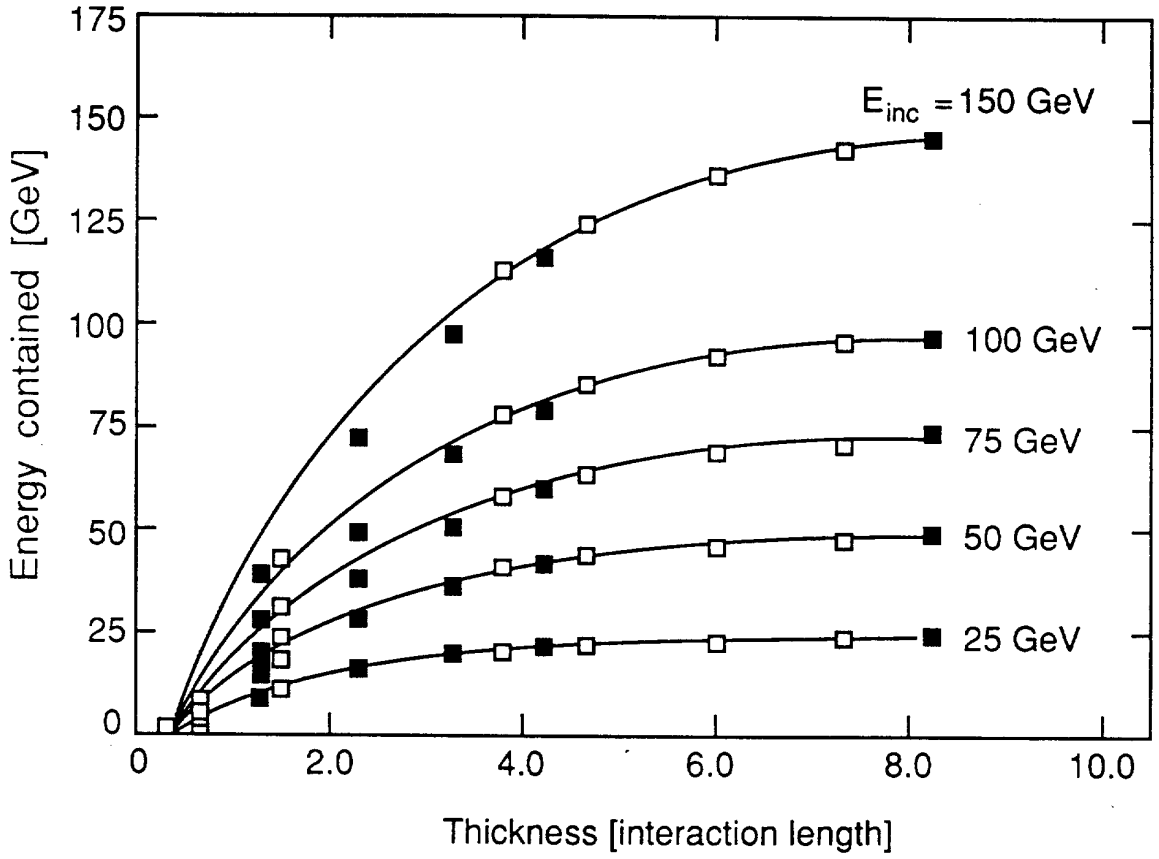
175
150
125
100
75
50
25
0
Energy contained [GeV]
0
2.0
4.0
6.0
8.0
10.0
Thickness [interaction length]
E_inc = 150 GeV
100 GeV
75 GeV
50 GeV
25 GeV

Fig 8

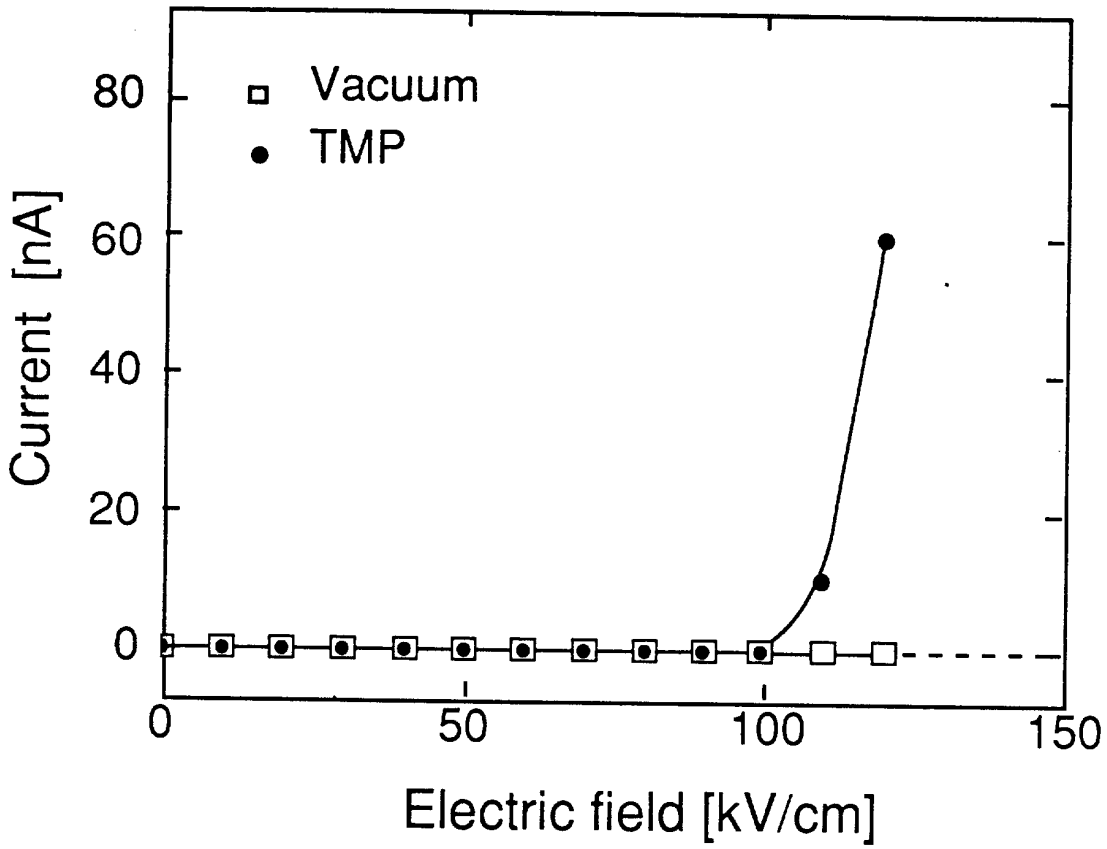
Vacuum
TMP
Current [nA]
80
60
40
20
0
0
50
100
150
Electric field [kV/cm]

Fig. 9

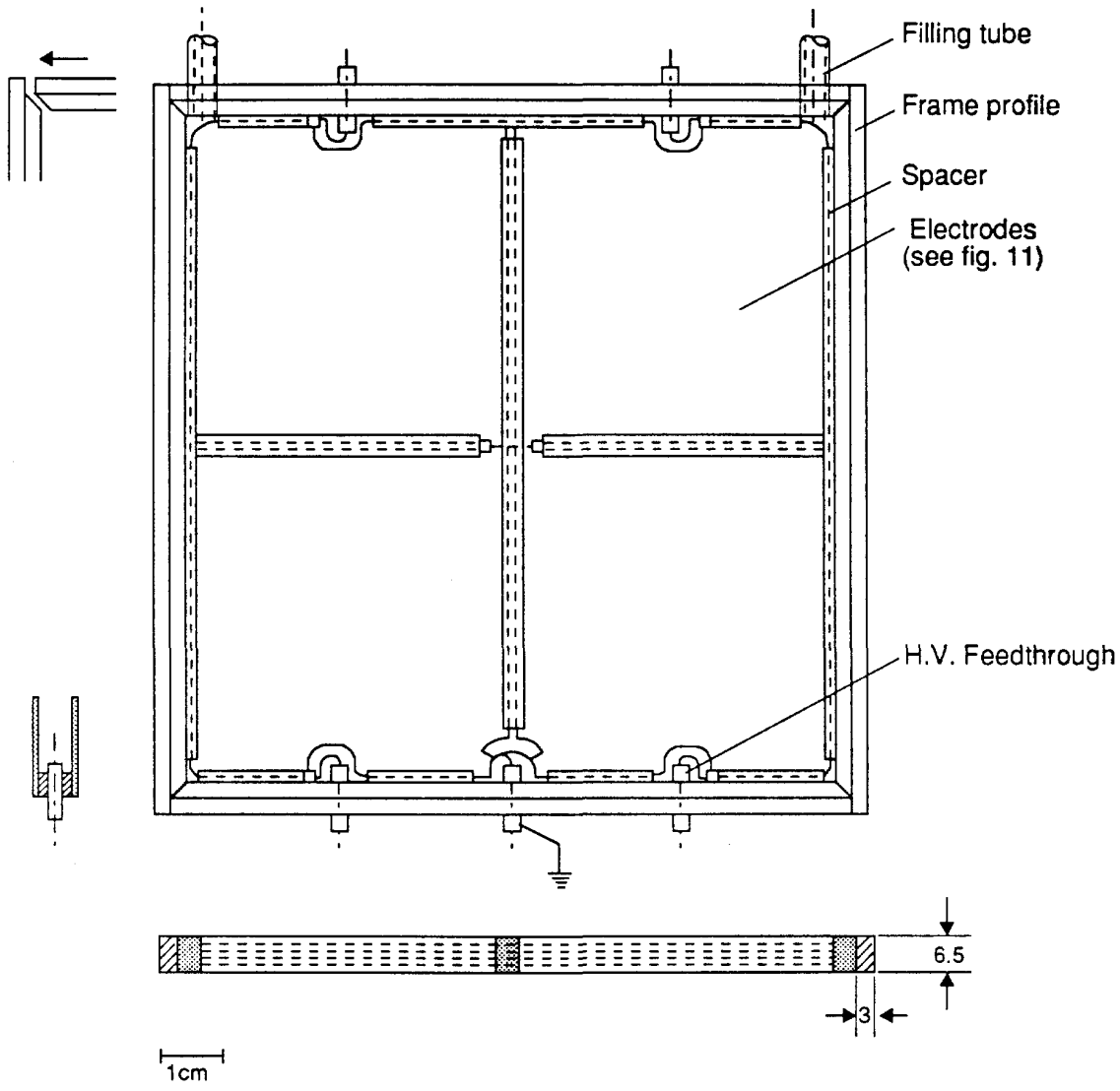
Filling tube
Frame profile
Spacer
Electrodes
(see fig. 11)
H.V. Feedthrough
6.5
3
1cm

Fig. 10

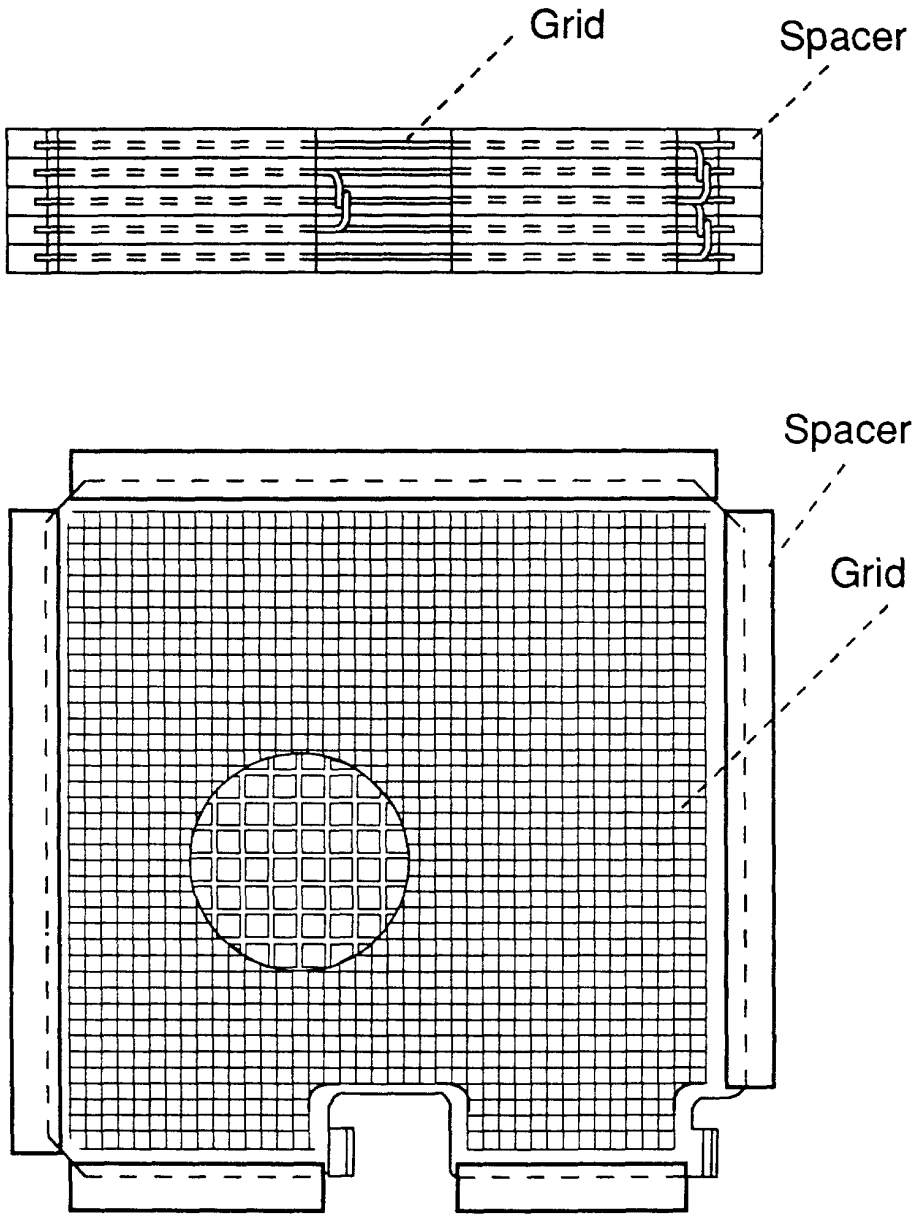

Fig. 11

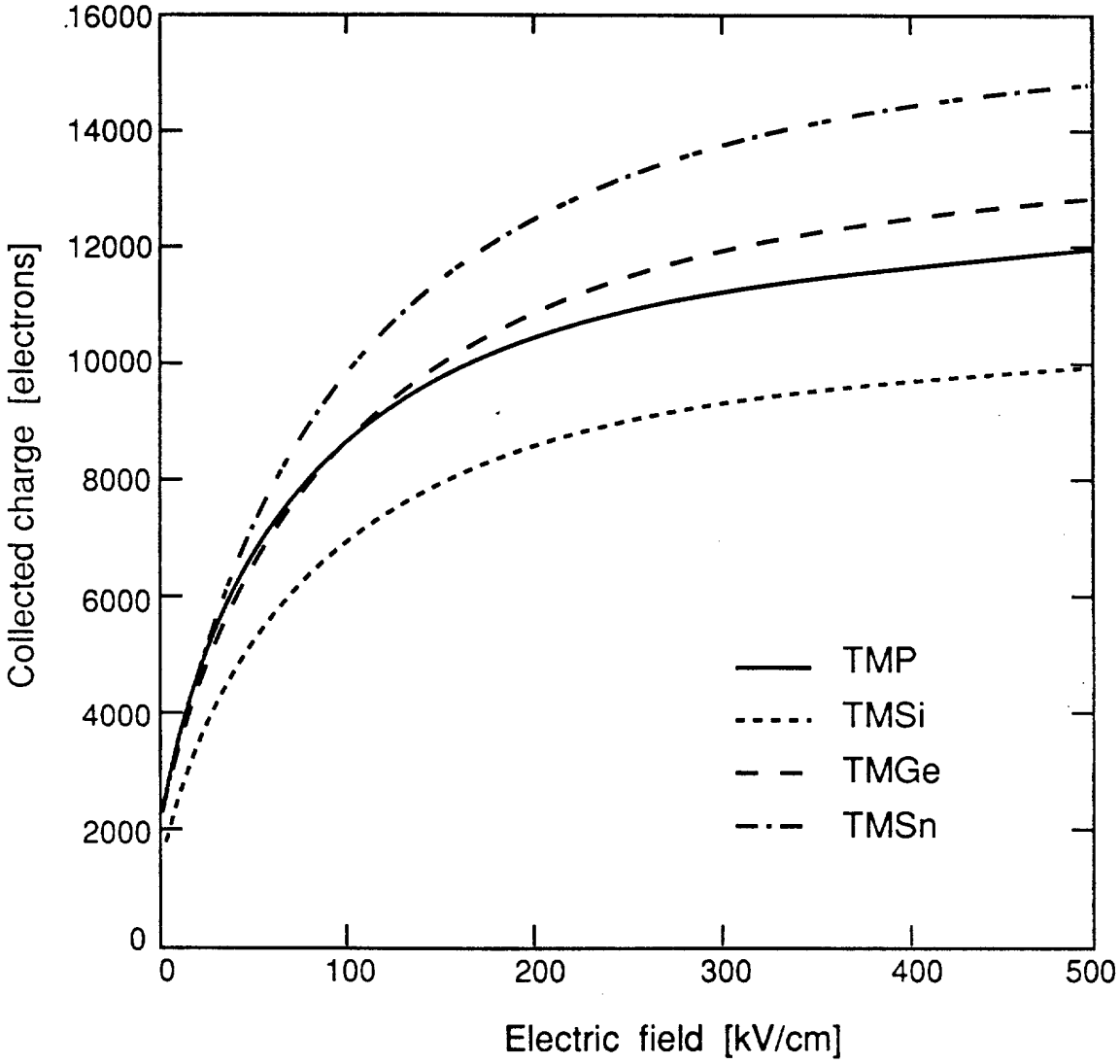
16000
14000
12000
10000
8000
6000
4000
2000
0
Collected charge [electrons]
0
100
200
300
400
500
Electric field [kV/cm]
TMP
TMSi
TMGe
TMSn

Fig. 12

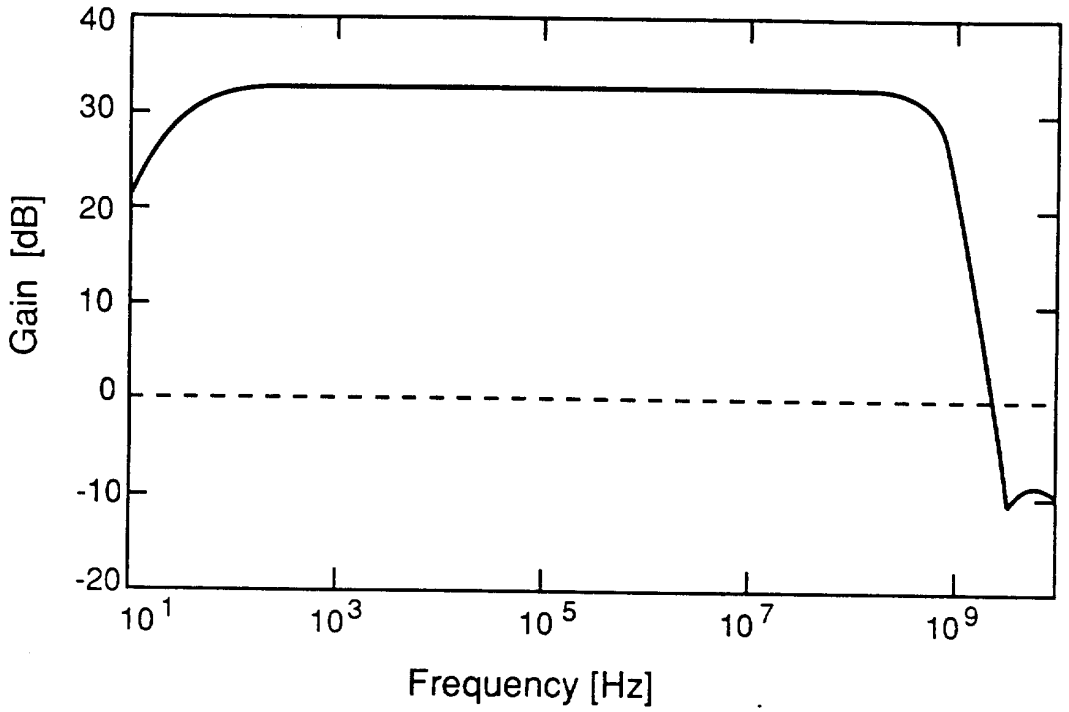

Fig. 13a

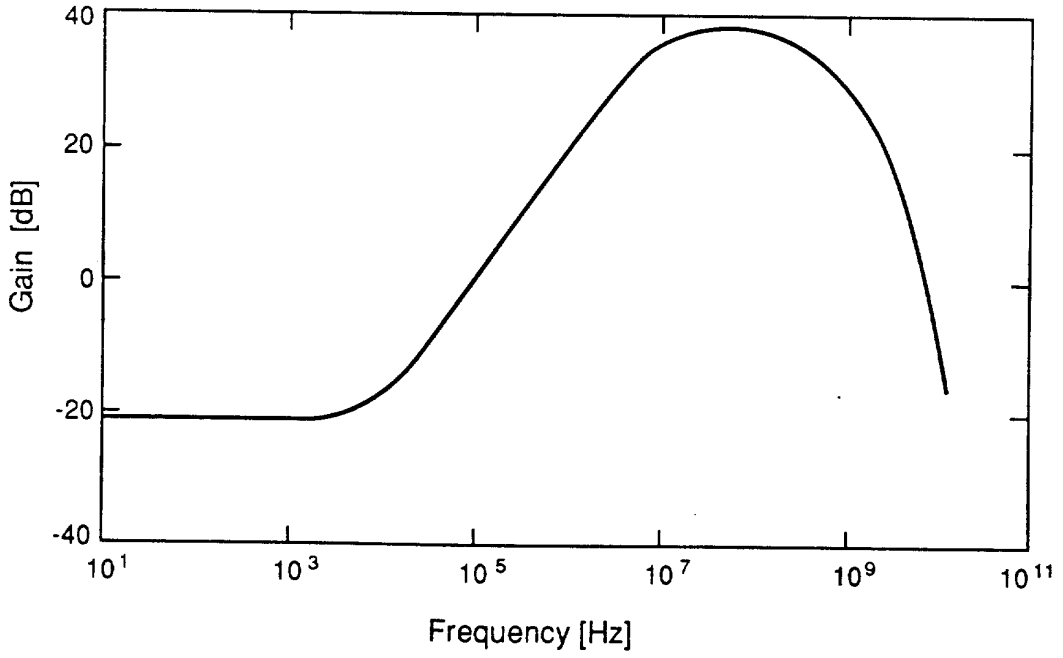

Fig. 13b

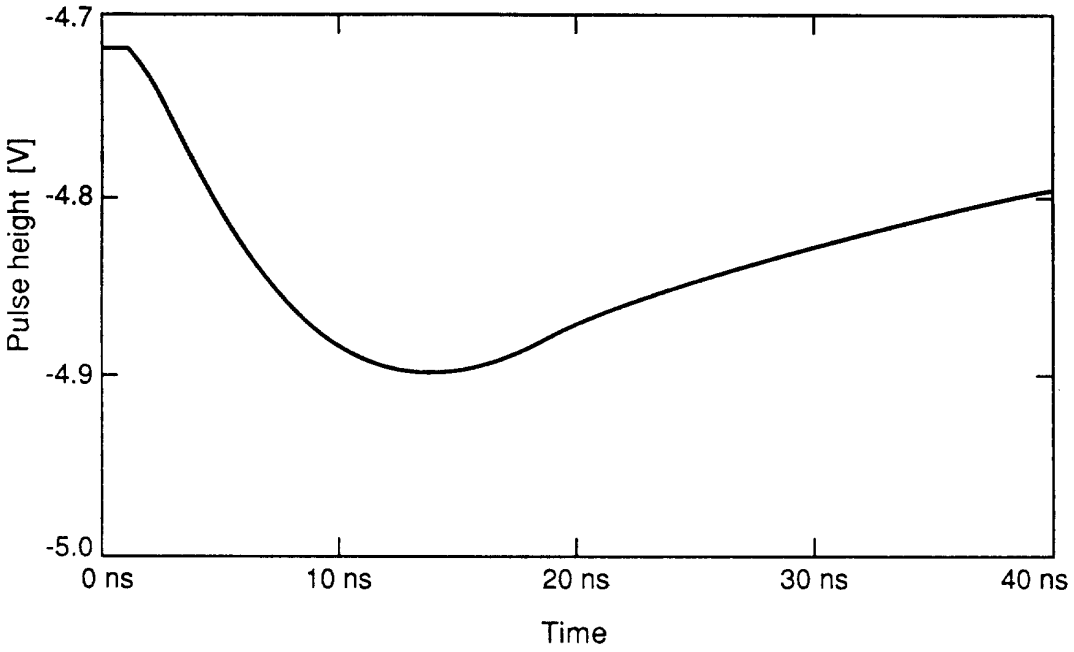

Fig. 14